



X-ray luminescence of ZnSCdS: Au, Cu phosphor using X-ray beams for medical applications

I. Kandarakis^a, D. Cavouras^{a,*}, C.D. Nomicos^b, G.S. Panayiotakis^c

^a Department of Medical Instrumentation Technology, TEI of Athens, Ag. Spyridonos Street, Aigaleo, 122 10 Athens, Greece

^b Department of Electronics, TEI of Athens, Ag. Spyridonos Street, Aigaleo, 122 10 Athens, Greece

^c Department of Medical Physics, Medical School, University of Patras, 265 00 Patras, Greece

Received 17 February 2000; received in revised form 31 August 2000

Abstract

The purpose of the present study was to evaluate the X-ray luminescence and imaging performance of phosphor screens prepared from ZnSCdS: Au, Cu. Absolute efficiency, X-ray luminescence efficiency, detector optical gain, and gain transfer function were experimentally determined. Theoretical models were also employed to fit experimental data and to determine optical properties of the phosphor material. Additionally, the emission spectrum of ZnSCdS: Au, Cu was measured and its compatibility with the spectral sensitivity of radiographic optical detectors (films, photodiodes) was determined. Results showed that ZnSCdS: Au, Cu is an efficient phosphor exhibiting high intrinsic X-ray to light conversion efficiency (0.17) and an excellent spectral compatibility (0.9) with amorphous silicon photodiodes, used in optical detectors of modern digital radiography systems. © 2001 Elsevier Science B.V. All rights reserved.

1. Introduction

Phosphors (or scintillators) are fluorescent materials emitting light when they interact with X-ray or γ -ray beams. These materials are used as radiation to light converters, in radiation detectors of various medical imaging systems (nuclear medicine, radiography, fluoroscopy, digital radiology, computed tomography). Phosphors are employed in the form of fluorescent layers, often

called phosphor screens, which are used in conjunction with an optical photon detector (radiographic film, photocathode, arrays of crystalline or amorphous silicon photodiodes, thin film transistors, CCDs etc.). The performance of fluorescent layers may be assessed by the determination of various parameters related to the quality of the phosphor-produced images. All these parameters depend on the intrinsic physical properties of the phosphor material (i.e. effective atomic number, density, intrinsic quantum structure, optical attenuation coefficients etc), which govern (1) the absorption of X-ray or γ -ray radiation, (2) the conversion of X-ray energy into light, and (3) the transmission of this light through the phosphor screen mass.

* Corresponding author. Present address: 37–39 Esperidon Street, Kallithea 17671, Athens, Greece. Tel.: +30-1-385-375 & +30-1-5385-372; fax: +30-1-5910-975.

E-mail addresses: cavouras@hol.gr, cavouras@ee.teiath.gr (D. Cavouras).

In the present study, the performance of ZnSCdS:Au,Cu phosphor, which has never been used in medical imaging, was evaluated under medical X-ray imaging conditions. The interest in studying this phosphor originates from the observation that materials based on ZnS host crystal structure often exhibit very high intrinsic conversion efficiency (conversion of incident radiation into light) relative to other phosphors. This is due to their low energy bandgap E_g (energy required to raise an electron from the valence to conduction band, $E_g < 4$ eV) [1,2]. This property facilitates the creation of electron–hole pairs, which then transfer energy to the crystal's luminescent centers to produce scintillations. ZnSCdS:Au,Cu has a medium time of fluorescence decay and, hence, it may only be considered for static imaging in radiographic detectors. The density of this material is 4.43 g/cm^3 , the K-absorption edge energies of Cd and Zn are 26.7 and 9.6 keV, respectively, while the corresponding atomic numbers are $Z = 48$ for Cd and $Z = 30$ for Zn. The values of the aforementioned intrinsic characteristics are comparable to those of other phosphors already in use in X-ray imaging; $\text{Y}_2\text{O}_2\text{S:Tb}$ has a density of 4.89 g/cm^3 , K-edge energy 17 keV, and the atomic number of Y is $Z = 39$. Barium based phosphors (BaSO_4 , BaFCl , BaPbSO_4) have densities ranging from 4 to 4.7 g/cm^3 , K-edge energy 37.4 keV and atomic number for Ba $Z = 56$. CsI:Na and CsI:Tl , used in non-granular screens of image intensifiers and in some digital imaging systems, have densities of 4.5 g/cm^3 . However, the characteristics of ZnSCdS:Au,Cu are lower than those of $\text{Gd}_2\text{O}_2\text{S:Tb}$, often employed in ordinary radiography having a density of 7.34 g/cm^3 , K-edge at 50.2 keV and $Z = 64$ for Gd [3–5]. All the aforementioned data indicate that ZnSCdS:Au,Cu could be a sufficient X-ray absorber at rather low X-ray energies as well as an efficient X-ray to light converter. The main difference between ZnSCdS:Au,Cu and ZnSCdS:Ag, which is used in image intensifiers, lies in their emission spectra. ZnSCdS:Au,Cu spectrum (550 nm) is slightly displaced, as compared to ZnSCdS:Ag (530 nm), towards longer wavelengths being better matched to the sensitivity of currently used amorphous or crystalline

silicon optical detectors of digital radiography systems.

To evaluate ZnSCdS:Au,Cu the following image quality parameters were determined:

1. The absolute efficiency (AE), which expresses the ability of a phosphor to convert incident X-ray exposure into emitted light energy [6–8].
2. The detector optical gain (DOG), which is defined by the number of emitted light photons (NEP) per X-ray. This conversion from energy into number of photons is useful in medical imaging since the statistics of these photons affect the information content of an image [9,10].
3. The gain transfer function (GTF), which combines optical gain with the modulation transfer function (MTF), the latter describing image contrast and spatial resolution [11]. GTF may be alternatively described as the optical gain defined in the spatial frequency domain.
4. The spectral matching factor (SMF) that describes how well the spectrum of the light emitted by the phosphor matches the spectral sensitivity of the optical photon detector [7,12].

2. Materials and methods

2.1. Theory and definitions

Absolute efficiency (η_A) has been defined [6,7] as the ratio of the light energy flux ($\dot{\Psi}$) emitted by an excited phosphor screen over the incident X-ray exposure rate (\dot{X}),

$$\eta_A = \frac{\dot{\Psi}_\lambda}{\dot{X}}. \quad (1)$$

In phosphor evaluation measurements, light energy flux is often expressed in $\mu\text{W/m}^2$ and exposure rate in mR/s, thus η_A is usually given in units of $[\mu\text{W s/mR m}^2]$, sometimes called efficiency units (E.U.) [7]. The latter provides a means to compare the performance of phosphor screens under experimental conditions. However, absolute efficiency does not clearly depict the fraction of X-ray beam energy that is useful to the imaging process. In order to represent screen efficiency as the useful fraction of energy (unitless quantity),

the incident exposure rate should be converted into X-ray energy flux $\dot{\Psi}_X$, also measured in $\mu\text{W}/\text{m}^2$. This may be done using the conversion formula [13,14]

$$\dot{\Psi}_X = \frac{\dot{X}}{[\mu_{\text{en}}/\rho]_A} \left[\frac{W_A}{e} \right], \quad (2)$$

where $[\mu/\rho]_A$ is the X-ray mass energy absorption coefficient for air [14], W_A is the average energy required to produce an ion pair in air and e is the electron charge. Thus, an additional physical parameter, the X-ray or γ -ray luminescence efficiency (η_ϕ), may be defined by the ratio

$$\eta_\phi = \frac{\dot{\Psi}_\lambda}{\dot{\Psi}_X}. \quad (3)$$

For the phosphor screens, usually employed in medical imaging, η_ϕ values range from 0.01 to 0.2 approximately.

The performance of phosphor screens may be alternatively estimated by the number of light photons emitted per incident X-ray photon. This number is called the detector optical gain, (G_O), given by the relation

$$G_O = \frac{\dot{\Phi}_\lambda}{\dot{\Phi}_X}, \quad (4)$$

where $\dot{\Phi}_\lambda$ and $\dot{\Phi}_X$ represent the emitted light photon flux and the incident X-ray photon flux (number of photons per unit of area and time), respectively. Photon fluxes may be obtained from energy fluxes by the following relations:

$$\dot{\Phi}_X = \dot{\Psi}_X/E \quad \text{and} \quad \dot{\Phi}_\lambda = \dot{\Psi}_\lambda/\hbar\omega, \quad (5)$$

where E is the mean energy of an X-ray photon and $\hbar\omega$ is the mean energy of a light photon. G_O values are of the order of 10^2 – 10^3 .

In addition to the aforementioned parameters, a phosphor screen's imaging performance may be described in the spatial frequency domain by the modulation transfer function. MTF describes the variation of image contrast with spatial frequency. Additionally MTF expresses spatial resolution, which is defined as the value of spatial frequency corresponding to $\text{MTF} = 0.05$ [15,16]. However, a complete description of the response of a phos-

phor screen to an input signal (X-ray beam) may be obtained by the gain transfer function [11] defined as

$$\text{GTF}(u) = G_O \text{MTF}(u), \quad (6)$$

where u denotes the spatial frequency. Since by definition [15,16], $\text{MTF} = 1$ for $u = 0$, the detector optical gain G_O may be considered as the zero frequency gain transfer function. GTF, as defined by relation (6), describes both the efficiency of a screen to emit light at low X-ray dose and the efficiency to produce high quality images, e.g. images of high contrast, spatial resolution and brightness.

AE, XLE and DOG may be theoretically determined using radiation transfer models based on optical properties of the phosphor materials [6,7,9,17]. In the context of these models the following formulas were developed:

$$\eta_A = \eta_\phi \left[\frac{1}{\mu_{\text{en}}} \right] \left(\frac{W_A}{e} \right), \quad (7a)$$

$$\begin{aligned} \eta_\phi(E_0, w_0) &= \int_0^{E_0} [d\Psi(E)/dE]_X \bar{\eta}_Q(E) \bar{\eta}_C \\ &\times \int_0^{w_0} \psi_R(E, w) \bar{G}_i(0, \sigma, \beta, \rho, w) dw dE, \end{aligned} \quad (7b)$$

$$\begin{aligned} G_O(E_0, w_0) &= \int_0^{E_0} [d\Phi(E)/dE]_X \bar{\eta}_Q(E) \bar{m}_0(E) \\ &\times \int_0^{w_0} \phi_R(E, w) \bar{G}_i(u, \sigma, \beta, \rho, w) dw dE, \end{aligned} \quad (7c)$$

where E_0 is the maximum energy of the X-ray energy flux spectral distribution $[d\Psi/dE]_X$ and X-ray photon flux spectral distribution $[d\Phi/dE]_X$. E_0 is numerically equal to the X-ray tube high voltage. w_0 is the coating weight of the phosphor screen, $\bar{\eta}_Q$ denotes the mean X-ray absorption efficiency averaged over the screen area, $\bar{\eta}_C$ is the intrinsic X-ray to light conversion efficiency, expressing the fraction of absorbed X-ray energy that is converted into light, \bar{m}_0 is the number of light photons created within the phosphor per

X-ray photon absorbed, \bar{G}_λ is a function expressing the fraction of light generated at an elementary thin layer dw at depth w that is transmitted through the phosphor screen. σ , β , ρ are optical parameters related to light absorption, light scattering and light reflectivity in the screen [6,7,9,17] (see Appendix A). The functions ψ_R and ϕ_R are probability distribution functions that describe the probabilities of X-ray energy and X-ray photon absorption, respectively, at an elementary thin layer dw at depth w from the phosphor surface (see Appendix A). The number m_0 may be expressed as a function of the intrinsic X-ray to light conversion efficiency and the energies of X-ray and light photons: $m_0(E) = \eta_C E / \hbar\omega$. According to (7c), the light transmission efficiency is a function of spatial frequency u [7,9]. Hence for $u \neq 0$, relation (7c) gives GTF while for $u = 0$, (7c) gives DOG or zero frequency GTF.

Another factor that is important to consider when a phosphor material is to be incorporated into a medical imaging detector, is the spectrum of the emitted light and its spectral compatibility with the sensitivities of various optical photon detectors. Spectral compatibility is often estimated by the spectral matching factor, which is defined as follows:

$$\text{SMS} = a_s = \frac{\int S_P(\lambda) S_D(\lambda) d\lambda}{\int S_D(\lambda) d\lambda}, \quad (8)$$

where S_P is the spectrum of the emitted light, S_D is the spectral sensitivity of the optical photon detector and λ denotes the light wavelength.

2.2. Experiments and calculations

The phosphor material ZnSCdS: Au, Cu was supplied in powder form from Derby Luminescents (code EPM). The mean phosphor grain size was approximately 7 μm . The phosphor screens were prepared by sedimentation of the phosphor powder on fused silica substrates. During sedimentation Na_2SiO_4 was used as binding material between the grains. Eight phosphor screens were prepared with coating weight ranging from 21 to 137 mg/cm^2 , corresponding to thickness ranging from 0.07 to 0.5 mm. To determine absolute effi-

ciency (η_A), X-ray luminescence efficiency (η_ϕ) and detector gain (G_O), the screens were excited to luminescence by irradiation with X-rays using X-ray tube voltages from 50 to 250 kVp. During excitation the light energy flux Ψ_λ was measured by an EMI 9558 photomultiplier coupled to a Cary 401 vibrating reed electrometer. Light was observed from the irradiated screen side (reflection mode technique) and from the non-irradiated one (transmission mode technique) [6,7,9,10]. In this way, both screens of a usual radiographic cassette were simulated.

To determine η_A the incident exposure rate was measured by a PTW (type no. 23333) ionization chamber dosimeter. For η_ϕ and G_O determination exposure data were converted into X-ray energy and X-ray photon flux data, Ψ_X and Φ_X , using relations (2) and (5), respectively.

Light photon flux Φ_λ was determined by relation (5) after determining the mean energy $\hbar\omega$ of light photons via emission spectrum measurements. The latter were performed using an Oriel 7440 grating monochromator.

MTF was determined by the square wave response function (SWRF) method [15,16] at 80 kVp. An SWRF test pattern (typ-53 of Nuclear Associates) comprising lead line pairs with spatial frequencies from 0.25 to 10 lp/mm was placed on the front side of the screens. The image of the test pattern was obtained on a radiographic film (Kodak Ortho GR), which was in contact with the backside of the screen [8,10]. This image was digitized on a Microtec Scanmaker II SP (1200 \times 1200 dpi) scanner. SWRF image patterns were obtained as image density variations along lines vertically directed with respect to the test pattern lines. These density variations were used to calculate MTF by the Coltman's formula [8,10].

Errors in absolute efficiency determination were mainly due to both light flux and exposure rate measurements and were of the order of 4%. Errors in MTF determination ranged between 0.7% and 3% depending on screen thickness and spatial frequency range. The X-ray unit used had a three phase generator with full-wave rectification, 5% ripple factor, 2 mm Al filter and HVL (Half Value Layer) equal to 2.5 mm Al at 80 kVp. HVL varied with kVp having values of 1.3 mm Al at 50 kVp,

2.9 mm Al at 100 kVp, 4.2 mm Al at 150 kVp. Furthermore, to simulate beam attenuation and X-ray spectrum modification by human body, X-rays were transmitted through an additional 20 mm Al filter before incidence on the phosphor screens.

3. Results and discussion

The variation of absolute efficiency with X-ray tube voltage is shown in Fig. 1 for three ZnSCdS:Au,Cu phosphor screens of 21, 94 and 121 mg/cm². Solid lines represent curves derived by fitting Eqs. (7a)–(7c) of the theoretical model, to the experimental data. The latter are depicted by points in Fig. 1. Best curve fitting was obtained using $\eta_C = 0.17$ and $\sigma = 33.8$ cm/g². The value of the reflectivity parameter β was found equal to 0.04. The value of η_C , as determined by the fitting, is higher than the corresponding values of CaWO₄ (0.05), often used in medical radiography screens, CsI:Na or CsI:Tl (0.10), used in image intensifiers and digital imaging detectors and NaI:Tl (0.15) used in nuclear medicine gamma cameras. It is also very close to the η_C values, previously found for the rare earth phosphors Gd₂O₂S:Tb and La₂O₂S:Tb, which range from 0.15 to 0.20 [3,7]. The values of σ and β , which depend on grain size and light wavelength, are very close to those found for other phosphors emitting in approximately the

same optical spectrum region (around 550 nm), e.g. for Gd₂O₂S:Tb, Y₂O₂S:Tb, La₂O₂S:Tb and Zn₂SiO₄:Mn phosphors, with the same grain size as ZnSCdS:Au,Cu and emitting principally at 545 and 530 nm, σ has been found equal to 30–38 cm/g² and β equal to 0.03, respectively [7,9]. The shape of the curves shown in Fig. 1 may be explained by considering the effects of X-ray and light photon interactions within a phosphor material. As is observed, absolute efficiency increases with increasing tube voltage, up to 60–70 kVp where its peak value was obtained. This behavior is mainly due to the presence of the photoelectric K-absorption edge of Zn (9.6 keV) and Cd (26.7 keV). As tube voltage increases, more photons of the X-ray beam spectrum acquire energies higher than 9.6 and 26.7 keV and, consequently, they are easily absorbed. Additionally, as tube voltage increases, larger amounts of X-ray energy are deposited within the phosphor mass and, hence, larger quantities of light are produced. As is observed, for tube voltages higher than 70 kVp absolute efficiency decreases rather rapidly with increasing kVp. This is because X-ray photons gradually acquire relatively high energies and become more penetrating. Thus, they are easier transmitted through the phosphor, without absorption and light creation.

To provide an estimation of the ZnSCdS:Au,-Cu X-ray absorption efficiency, the latter was calculated as function of energy, using the X-ray

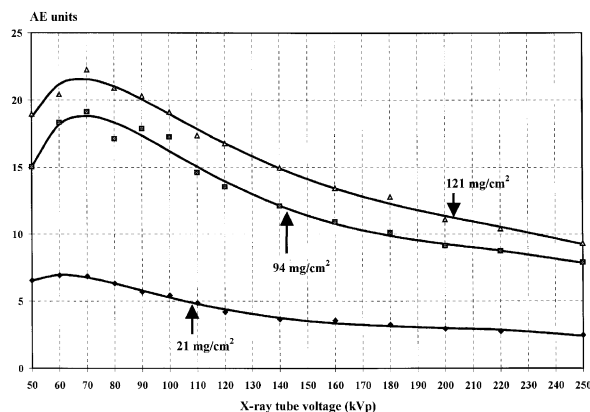


Fig. 1. Variation of absolute efficiency (AE) with X-ray tube voltage for 21, 94 and 121 mg/cm² ZnSCdS:Au,Cu phosphor screens. Points: experimental data; solid lines: fitted curves. AE units $\mu\text{W s/mR m}^2$.

energy absorption coefficient [18] and the exponential law of X-ray attenuation (see Appendix A). For energies in the range between 30 and 50 keV, ZnSCdS:Cu was found to be a better X-ray absorber than $\text{Gd}_2\text{O}_2\text{S:Tb}$, often used in current radiographic detectors (with K-edge of Gd at 50.2 keV). At 50 keV, corresponding approximately to the mean energy of an 80 kVp X-ray beam, and for 80 mg/cm^2 screens, the absorption efficiency of ZnSCdS:Cu was found equal to 0.25. This is about 20% higher than that of $\text{Gd}_2\text{O}_2\text{S:Tb}$, calculated under the same conditions. However, $\text{Gd}_2\text{O}_2\text{S:Tb}$ exhibits a sudden absorption increase just after 50 keV.

Fig. 2 shows the variation of absolute efficiency with increasing phosphor-coating weight. Two efficiency curves are depicted corresponding to transmission and reflection modes of measurement. The values obtained in reflection mode were found higher than those measured in transmission mode. This is explained by considering that, due to the exponential law of X-ray absorption, more X-ray energy is deposited within the first half of screen thickness than in the second half. Thus, light photons created at points of X-ray absorption, travel shorter distances when they escape the screen from the side facing the X-ray source than from the other side. Consequently larger amounts of light are collected in reflection mode than in transmission mode measurements. Absolute efficiency, in both transmission and reflection modes, increases with increasing phosphor thickness. However, for coating weight thicker

than $110\text{--}120 \text{ mg/cm}^2$ absolute efficiency shows a tendency to saturate or to decrease. This variation is in accordance with the X-ray absorption mechanism, which imposes that larger amounts of the incident X-ray energy are absorbed when phosphor thickness increases. This results in higher light flux emission in thick screens. Furthermore, as phosphor mass increases, the effects of light absorption and light scattering within the phosphor material become more important, resulting in attenuation of light and hence in absolute efficiency reduction, giving the saturation effect at $120\text{--}140 \text{ mg/cm}^2$.

The results concerning X-ray luminescence efficiency and detector gain (relations (3) and (4), respectively) are plotted in Figs. 3 and 4, respectively. The shapes of these curves differ slightly from the shapes of the absolute efficiency curves due to the corresponding differences in the definitions of XLE and DOG. For example, DOG expresses the number of emitted light photons while absolute efficiency describes the emitted light energy flux. Additionally, the denominator of absolute efficiency in relation (1) gives the exposure, which is affected by the X-ray absorption properties of air [13,14], while the denominators of XLE in relation (3) and of DOG in relation (4) give the incident X-ray energy flux and the number of X-ray photons, respectively.

Fig. 5 shows GTF curves for the 21, 94, 121 mg/cm^2 screens determined at 80 kVp. In accordance with data shown in Fig. 4, the thin screen of 21 mg/cm^2 exhibits very low zero

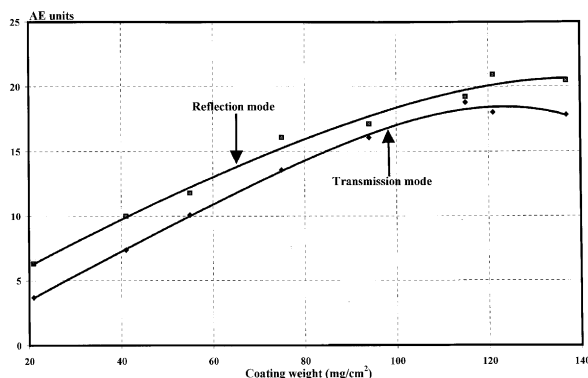


Fig. 2. Variation of absolute efficiency (AE) with phosphor coating weight measured at 80 kVp. AE units: $\mu \text{W s/mR m}^2$.

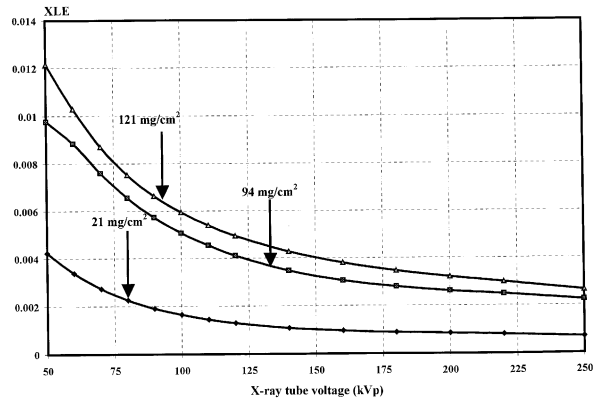


Fig. 3. Variation of X-ray luminescence efficiency (XLE) with X-ray tube voltage for 21, 94 and 121 mg/cm² ZnSCdS: Au, Cu phosphor screens.

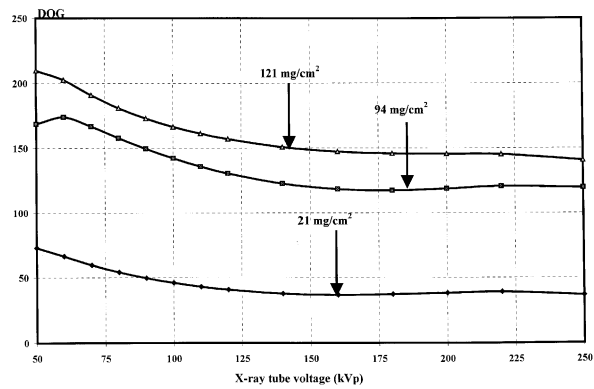


Fig. 4. Variation of detector optical gain (DOG) with X-ray tube voltage for 21, 94 and 121 mg/cm² ZnSCdS: Au, Cu phosphor screens.

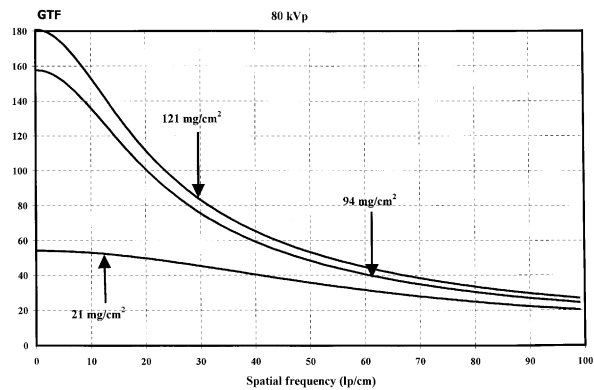


Fig. 5. Gain transfer function (GTF) of 21, 94 and 121 mg/cm² ZnSCdS: Au, Cu phosphor screens determined at 80 kVp.

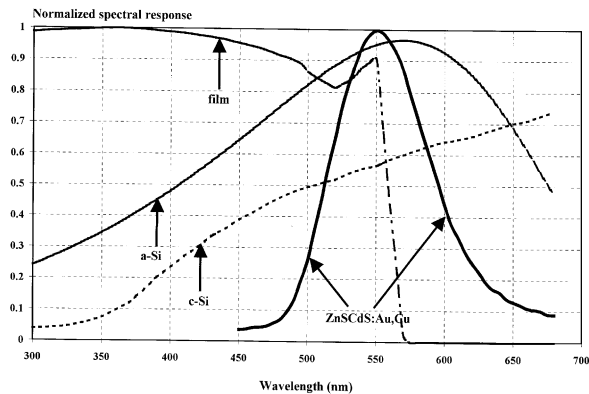


Fig. 6. Normalized ZnSCdS:Cu,Au emitted light spectrum and spectral sensitivity curves of c-Si, a-Si and orthochromatic film.

frequency GTF value, but it decreases very slowly with spatial frequency. On the contrary, thicker screens showed considerably higher zero frequency values but they decreased very rapidly towards the high frequency range. The shape of the GTF curves corresponding to the medium and high frequency ranges is strongly affected by the isotropic light production and the light scattering effects within the phosphor. Both these factors cause a widening in the distribution of light photons arriving at the emitting surface of the phosphor. This widening is more pronounced in thick screens, since laterally directed light photons are projected in a larger screen area than in the case of thin screens. Hence MTF, which expresses light spread in the spatial frequency domain, is lower in thick screens and affects GTF in a similar way. This explains why the GTF of thin screens exhibits a rather slow variation at medium and high frequencies.

Fig. 6 shows the spectrum of the light emitted by the ZnSCdS:Cu,Au phosphor together with spectral sensitivity curves of some optical photon detectors used in combination with the phosphor material in medical imaging systems. These detectors are the following: (1) crystalline silicon (c-Si) which is used in CCD arrays of some digital radiography detectors, (2) amorphous silicon (a-Si) used in modern flat panel digital radiography detectors, (3) orthochromatic film employed in conventional radiographic cassettes. The data shown in the figure indicate that there is excellent

coincidence between the spectrum and the sensitivity of the a-Si detector. As is also observed, the light spectrum is situated well within the upper and lower wavelength limits of the c-Si spectral sensitivity curve. This indicates that ZnSCdS:Cu,Au could be conveniently incorporated in currently used medical radiography systems.

Table 1 shows the values of spectral matching factors corresponding to various phosphor-optical photon detector combinations. It is worth noting the very high matching factor (0.9) of ZnSCdS:Cu,Au with the amorphous silicon spectral sensitivity. Additionally, for both c-Si and a-Si, ZnSCdS:Cu,Au showed values higher than CsI and Gd₂O₂S:Tb, which are widely used in medical imaging. Accordingly it could be concluded that the ZnSCdS:Cu,Au phosphor is very well matched with the sensitivity of the optical photon detectors employed in modern digital radiography X-ray detectors.

Table 1
Spectral matching factors for phosphor-optical detector combinations

	ZnSCdS:Cu,Au	Gd ₂ O ₂ S:Tb	CsI:Na
c-Si	0.577	0.533	0.309
a-Si	0.900	0.875	0.578
Orthochromatic film	0.500	0.709	0.943
GaAs photocathode	0.941	0.937	0.917

Acknowledgements

This study is dedicated to the memory of Prof. G.E. Giakoumakis, leading member of our team, whose work on phosphor materials has inspired us to continue.

Appendix A

The light transmission efficiency of a phosphor screen may be expressed by the following integral:

$$\overline{G}_\lambda(u, w_0) = \int_0^{w_0} \psi_R(E, w) \overline{G}_\lambda(u, w) dw. \quad (\text{A.1})$$

$\overline{G}_\lambda(u, w)$ is a function representing the fraction of light energy flux, generated after the absorption of an X-ray photon at depth w within the screen, that escapes the phosphor mass. The function $\psi_R(E, w)$ describes the relative probability of X-ray energy absorption at an elementary thin phosphor layer dw lying at depth w from the screen surface, given as

$$\psi_R(E, w) = \frac{\overline{\Psi}_X(E) \mu(E) \exp[-\mu(E)w] dw}{\int_0^{w_0} \overline{\Psi}_X(E) \mu(E) \exp[-\mu(E)w] dw}, \quad (\text{A.2})$$

where the numerator is equal to X-ray energy absorbed at the thin layer dw at depth w and the denominator is equal to the X-ray energy absorbed within the whole phosphor screen. $\overline{\Psi}_X(E)$ is the mean X-ray energy flux incident on the screen and averaged over the surface of the screen and $\mu(E)$ is the X-ray energy absorption coefficient of the phosphor material [18]. The denominator of Eq. (A.2) divided by $\overline{\Psi}_X$ equals to the X-ray absorption efficiency of the phosphor screen, $\overline{\eta}_Q$, in Eq. (7b).

The function $\overline{G}_\lambda(u, w)$ has been defined as a solution to a photon diffusion differential equation [17], which describes the propagation of light through light scattering media, and it is given as follows:

$$\overline{G}_\lambda(u, w) = \frac{\rho_1[(\beta + \rho_0)e^{\sigma w} + (\beta - \rho_0)e^{-\sigma w}]}{(\beta + \rho_0)(\beta + \rho_1)e^{\sigma w_0} - (\beta - \rho_0)(\beta - \rho_1)e^{-\sigma w_0}}, \quad (\text{A.3})$$

where σ is an optical parameter of the phosphor material which is equal to the reciprocal of the light photon diffusion length [6,7,17] and it is given as a function of the optical scattering coefficient s and the optical absorption coefficient a ,

$$\sigma = [a(a + 2s)]^{1/2}, \quad (\text{A.4})$$

ρ_0, ρ_1 are optical parameters expressing the reflection of light at the front and back screen surfaces and they are defined as

$$\rho_n = (1 - r_n)/(1 + r_n), \quad n = 0, 1, \quad (\text{A.5})$$

where r_n denotes the optical reflection coefficients at the front and back screen surfaces.

β is an optical parameter which is equal to ρ corresponding to the case of a very thick screen with no light transmission through it. β has been also expressed as a function of a and s [6,7],

$$\beta = [a/(a + 2s)]^{1/2}. \quad (\text{A.6})$$

In relation (7c), the light transmission efficiency was expressed in terms of the function $\phi_R(E, w)$, which is defined as follows:

$$\phi_R(E, w) = \frac{\overline{\Phi}_X(E) \mu(E) [\exp(-\mu(E)w)] dw}{\int_0^{w_0} \overline{\Phi}_X(E) \mu(E) [\exp(-\mu(E)w)] dw}, \quad (\text{A.7})$$

where $\overline{\Phi}_X(E)$ denotes the mean X-ray photon flux incident on the screen surface and averaged over the screen area. ϕ_R expresses the relative probability of an X-ray photon absorption at an elementary thin layer dw at depth w within the screen. The calculations of $\overline{\Psi}_X(E)$ in Eq. (A.2), $\overline{\Phi}_X(E)$ in Eq. (A.7) and of the spectral distributions in relation (7a)–(7c) were based on published models [19]. Fitting of absolute efficiency experimental data was performed employing the Levenberg–Marquard method [20].

References

- [1] R.C. Alig, S. Bloom, J. Electrochem. Soc. 124 (1977) 1136.
- [2] G. Blasse, J. Lumin. 60 (1994) 930.
- [3] B.A. Arnold, The Physics of Medical Imaging: Recording System, Measurements and Techniques, American Association of Physicists in Medicine, New York, 1979.

- [4] G. Zweig, D.A. Zweig, SPIE 419 (1983) 297.
- [5] A.M. Gurvich, Radiat. Meas. 24 (1995) 325.
- [6] G.W. Ludwig, J. Electrochem. Soc. 118 (1971) 1152.
- [7] I. Kandarakis, D. Cavouras, G.S. Panayiotakis, C.D. Nomicos, Phys. Med. Biol. 42 (1997) 1351.
- [8] D. Cavouras, I. Kandarakis, P. Prassopoulos, E. Kanellopoulos, C.D. Nomicos, G.S. Panayiotakis, Acta Radiol. 40 (1999) 211.
- [9] I. Kandarakis, D. Cavouras, P. Prassopoulos, E. Kanellopoulos, C.D. Nomicos, G.S. Panayiotakis, Appl. Phys. A 67 (1998) 521.
- [10] I. Kandarakis, D. Cavouras, N. Kalivas, C.D. Nomicos, G.S. Panayiotakis, Nucl. Instr. and Meth. B 155 (1999) 199.
- [11] D. Cavouras, I. Kandarakis, T. Maris, G.S. Panayiotakis, C.D. Nomicos, Eur. J. Radiol. 35 (1999) 70.
- [12] D. Cavouras, I. Kandarakis, P. Prassopoulos, E. Kanellopoulos, C.D. Nomicos, G.S. Panayiotakis, Technol. Health Care 7 (1999) 53.
- [13] J.R. Greening, Fundamentals of Radiation Dosimetry. Institute of Physics, London, 1985, p. 56.
- [14] W.R. Hendee, Medical Radiation Physics. Year Book Medical Publishers, Chicago, 1970, p. 145.
- [15] ICRU, Modulation transfer function of screen-film systems, ICRU Report 41, 1986.
- [16] G.T. Barnes, The Physics of Medical Imaging: Recording System, Measurements and Techniques, American Association of Physicists in Medicine, New York, 1979.
- [17] R.K. Swank, Appl. Opt. 12 (1973) 1865.
- [18] E. Storm, H. Israel, Photon cross-sections from 0.001 to 100 MeV for elements 1 through 100, Report LA-3753, Los Alamos Scientific Laboratory, University of California, 1967.
- [19] D.M. Tucker, G.T. Barnes, D.B. Chakraborty, Med. Phys. 18 (1991) 211.
- [20] W.H. Press, B.P. Flannery, S.A. Teukolsky, W.T. Vetterling, in: Numerical Recipes in C: The Art of Scientific Computing, Cambridge University Press, 1990, p. 542.